Supplementary Information for *Chemical Communications*

Theoretical limits of electron and hole doping in single-layer graphene from DFT calculations

Dawid Ciszewski, Wojciech Grochala*

Centre of New Technologies, University of Warsaw, Banacha 2C St., 02-097 Warsaw, Poland

Table of Contents

1. Computational details 3
2. Electronic Dispersion and DOS from +20% (hole doping) to -200% (electron doping) 5
3. C–C bond length vs doping level 8
4. Lattice constant vs doping level 8
5. References 9

1. Computational details

DTF calculations leading to investigation of dynamic stability in monolayer graphene under different doping levels from 0.2 hole per atom up to 2.0 electron per atom with a calculation step of 0.1 hole/electron was performed in two stages. Firstly, relaxation with regard to total energy and forces was conducted to find the relaxed structure in the ground state. The second step involved calculation of the electronic dispersion and DOS, phononic dispersion and critical temperature $T_{c.}$ All calculations were performed using the Quantum ESPRESSO (QE) suite[1,2] with Perdew-Burke-Ernzerhof (PBE) optimized norm-conserving Vanderbilt (ONCV) pseudopotentials[3,4] from the Pseudo Dojo library[5]. A plane-wave kinetic energy cutoff was set to 100 Ry for the wavefunctions and 400 Ry for the charge density and potential. Brillouin-zone integration involved a 18x18x1 Γ-centered k-mesh with a Methfessel-Paxston smearing width[6] of 0.02 Ry. Since monolayer graphene is a 2D material, the out-of-plane direction was sampled with only one k-point with a vacuum slab of at least 10 Å, which was added to ensure proper periodic boundary conditions. Structural optimization was considered converged when the total energy and atomic forces per atom reached tolerances of 10^{-6} Ry and 10^{-4} Ry/Å, respectively. The vacuum spacing was kept constant. Monolayer graphene was doped both by electrons and holes until dynamic instability (i.e., the appearance of imaginary phonon modes) was reached. The dynamical matrices and linear variation of the self-consistent potential were computed using density-function perturbation theory (DFPT)[7] on the irreducible set of a regular 6x6x1 q-mesh. For each q-point, the electron-phonon matrix elements were calculated on a denser 60x60x1 k-mesh. The Eliashberg spectral function was calculated for a set of broadening ranging from 0 to 0.05 Ry. The superconducting critical temperature was determined using the Allen-Dynes modified McMillan formula[8], assuming a Coulomb pseudopotential of $\mu = 0.10$ and at degauss value of 0.03. The Eliashberg spectral function (α^2F), electron-phonon coupling strength (λ), logarithmic average phonon frequency (ω_{log}), and superconducting temperature (T_c) formulas are shown below.

$$\alpha^2F(\omega) = \frac{1}{N_F}\int\frac{dkdq}{\Omega_{BZ}^2}\sum_{mnv}\left|g_{mnv}(k,q)\right|^2\delta\left(\epsilon_{nk} - \epsilon_F\right)\delta\left(\epsilon_{mk+q} - \epsilon_F\right)\delta\left(\hbar\omega - \hbar\omega_{qv}\right)$$

$$\lambda = 2\int_0^\infty\frac{\alpha^2F(\omega)}{\omega}d\omega$$

$$\omega_{log} = exp\left[\frac{2}{\lambda}\int_0^\infty d\omega\frac{\alpha^2F(\omega)}{\omega}log\omega\right]$$

The Eliashberg spectral function ($\alpha^2F(\omega)$), the electron phonon coupling strength (λ), the logarithmic frequency (ω_{log}), and ω_2 are used to calculate the critical temperature through the modified Allen-Dynes modified McMillan formula:

$$k_BT_c = \frac{\hbar\omega_{log}}{1.2}exp\left[-\frac{1.04(1+\lambda)}{\lambda - \mu^*(1+0.62\lambda)}\right]$$

To add a chemical picture of bonding and antibonding interactions, projected and integrated crystal orbital Hamilton population (COHP) calculations were performed using LOBSTER (Local-Orbital Basis Suite Towards Electronic-Structure Reconstruction) software package.[9,10] The projection of the DFT wavefunctions onto a localized atomic orbital basis employed the Bunge basis set. This basis comprises numerical atomic orbitals derived from nonrelativistic Hartree–Fock calculations of free atoms, following the parameterization of Bunge *et al.*[11] It is worth mentioning that the study considered highly doped graphene, leading to high total charge spilling values of up to % at the most extreme doping levels. Orbital-resolved electron populations were recovered correctly at all doping levels.

The following sections present electronic band structure, electronic DOS, as well as lattice constants and C–C bond lengths as functions of the doping level ranging from 0.2 holes per atom to 2 electrons per atom. For reference, ±100% doping corresponds to 1 hole (+) (electron (-)) per atom.

2. Electronic Dispersion and DOS from +20% (hole doping) to -200% (electron doping)

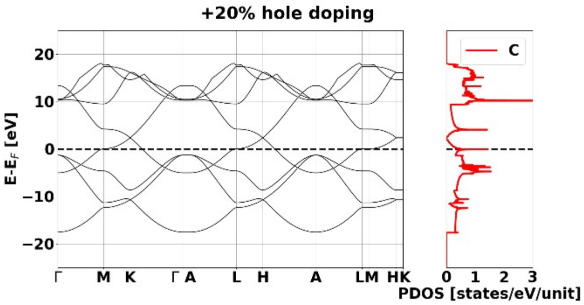
+20% hole doping

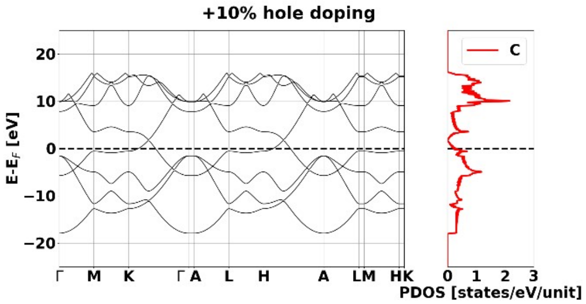
+10% hole doping

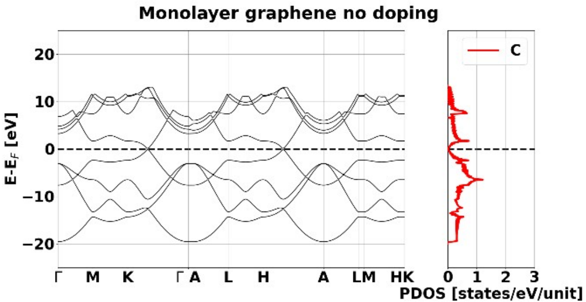
Monolayer graphene no doping

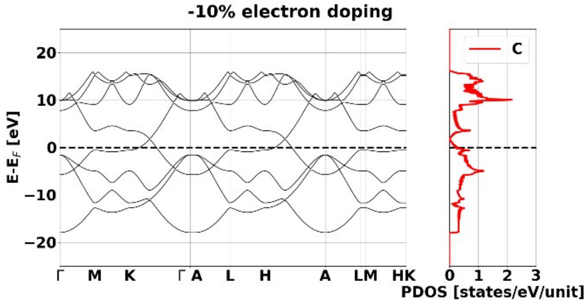

-10% electron doping

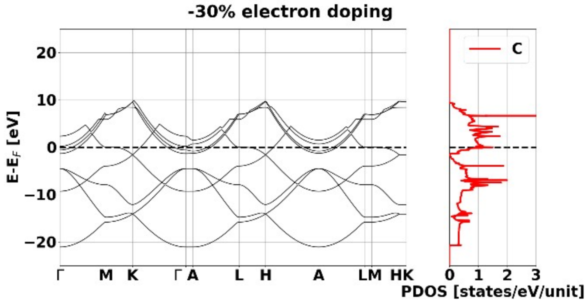

-30% electron doping

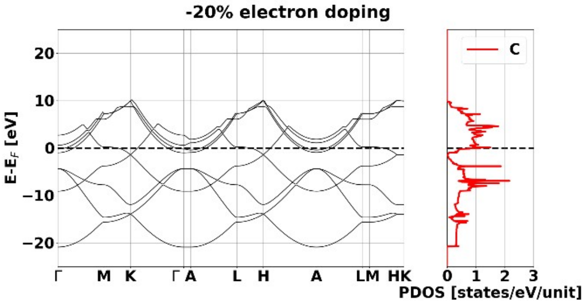

-20% electron doping

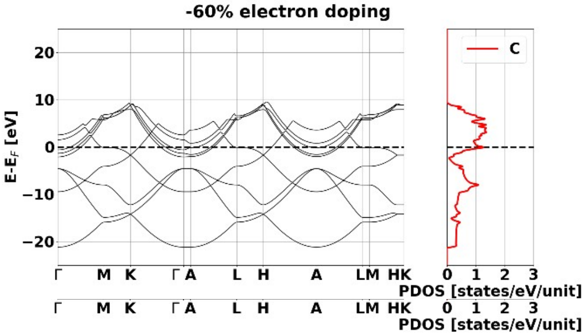

-60% electron doping

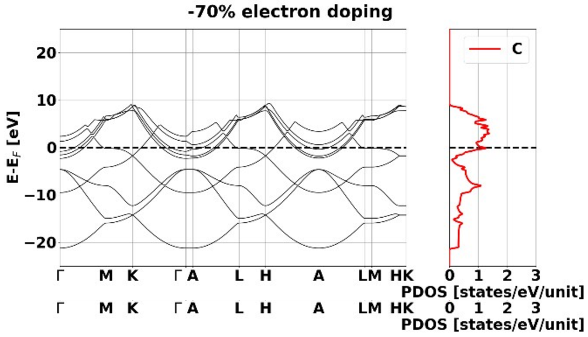

-70% electron doping

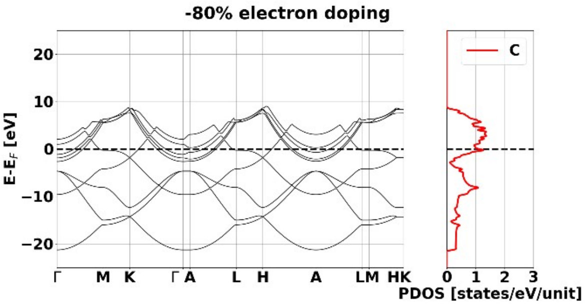
-80% electron doping

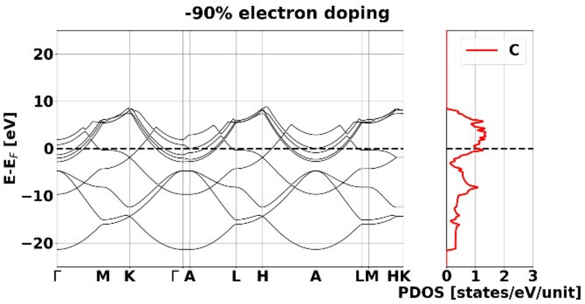
-90% electron doping

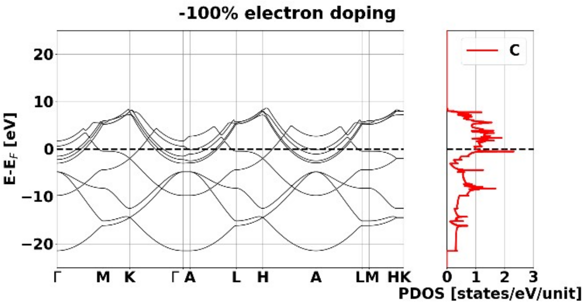
-100% electron doping

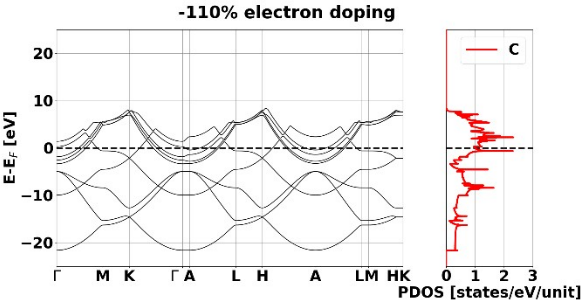
-110% electron doping

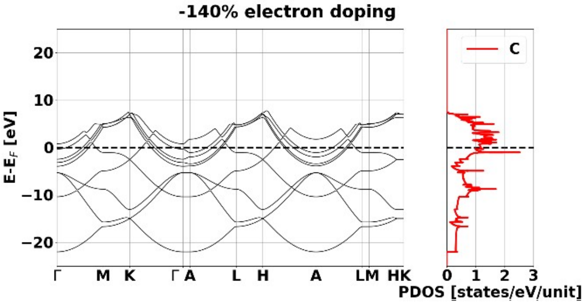
-140% electron doping

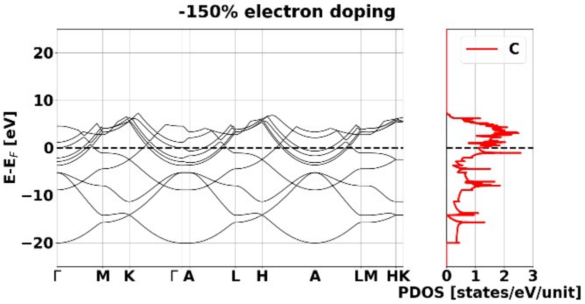
-150% electron doping

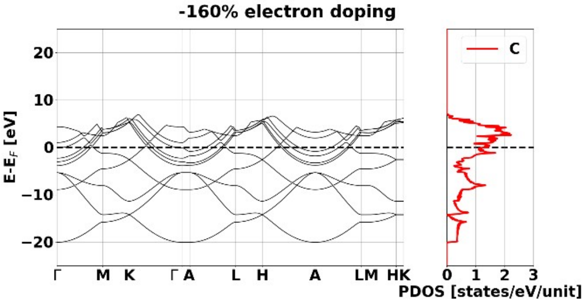
-160% electron doping

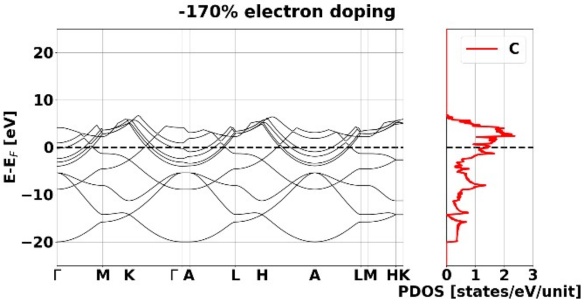
-170% electron doping

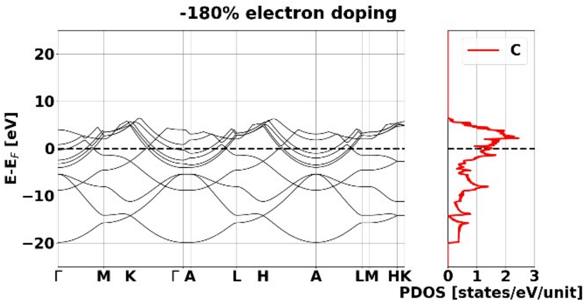

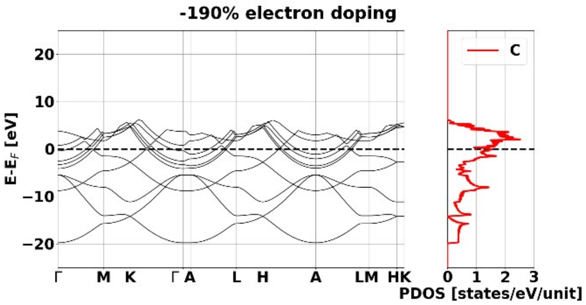

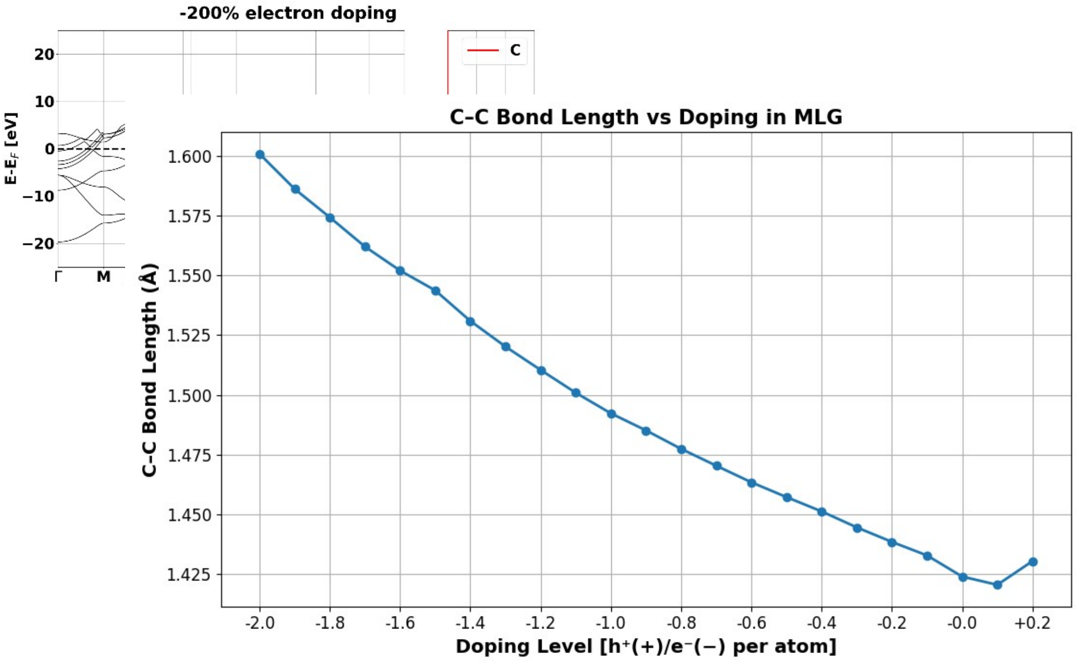

3. C–C bond length vs doping level

4. Lattice constant vs doping level

Doping [h$^+$(+)/e$^-$(-)	+0.2	+0.1	0	-0.1	-0.2	-0.3	-0.4	-0.5	-0.6	-0.7	-0.8	-0.9

per atom]											
Lattice constant *a* in MLG [Å]	**2.478**	**2.460**	**2.467**	**2.482**	**2.492**	**2.502**	**2.514**	**2.524**	**2.535**	**2.548**	**2.559**	**2.572**

-1.0	**-1.1**	**-1.2**	**-1.3**	**-1.4**	**-1.5**	**-1.6**	**-1.7**	**-1.8**	**-1.9**	**-2.0**
2.585	**2.600**	**2.616**	**2.633**	**2.652**	**2.675**	**2.688**	**2.706**	**2.767**	**2.747**	**2.773**

5. References

(1) P. Giannozzi, S. Baroni, N. Bonini, M. Calandra, R. Car, C. Cavazzoni, D. Ceresoli, G. L. Chiarotti, M. Cococcioni, I. Dabo, A. Dal Corso, S. De Gironcoli, S. Fabris, G. Fratesi, R. Gebauer, U. Gerstmann, C. Gougoussis, A. Kokalj, M. Lazzeri, L. Martin-Samos, N. Marzari, F. Mauri, R. Mazzarello, S. Paolini, A. Pasquarello, L. Paulatto, C. Sbraccia, S. Scandolo, G. Sclauzero, A. P. Seitsonen, A. Smogunov, P. Umari and R. M. Wentzcovitch, *J. Phys. Condens. Matter*, 2009, **21**, 395502.

(2) P. Giannozzi, O. Andreussi, T. Brumme, O. Bunau, M. Buongiorno Nardelli, M. Calandra, R. Car, C. Cavazzoni, D. Ceresoli, M. Cococcioni, N. Colonna, I. Carnimeo, A. Dal Corso, S. De Gironcoli, P. Delugas, R. A. Distasio, A. Ferretti, A. Floris, G. Fratesi, G. Fugallo, R. Gebauer, U. Gerstmann, F. Giustino, T. Gorni, J. Jia, M. Kawamura, H. Y. Ko, A. Kokalj, E. Kücükbenli, M. Lazzeri, M. Marsili, N. Marzari, F. Mauri, N. L. Nguyen, H. V. Nguyen, O. Otero-De-La-Roza, L. Paulatto, S. Poncé, D. Rocca, R. Sabatini, B. Santra, M. Schlipf, A. P. Seitsonen, A. Smogunov, I. Timrov, T. Thonhauser, P. Umari, N. Vast, X. Wu and S. Baroni, *J. Phys. Condens. Matter*, 2017, **29**, 465901.

(3) J. P. Perdew, K. Burke and M. Ernzerhof, *Phys. Rev. Lett.*, 1996, **77**, 3865–3868.

(4) J. P. Perdew, K. Burke and M. Ernzerhof, *Phys. Rev. Lett.*, 1997, **78**, 1396.

(5) D. R. Hamann, *Phys. Rev. B*, 2013, **88**, 085117.

(6) M. Methfessel and A. T. Paxton, *Phys. Rev. B*, 1989, **40**, 3616–3621.

(7) S. Baroni, S. De Gironcoli, A. Dal Corso and P. Giannozzi, *Rev. Mod. Phys.*, 2001, **73**, 515–562.

(8) S. Grimme, J. Antony, S. Ehrlich and H. Krieg, *J. Chem. Phys.*, 2010, **132**, 154104.

(9) R. Dronskowski and P. E. Blöchl, *J. Phys. Chem.*, 1993, **97**, 8617–8624.

(10) R. Nelson, C. Ertural, J. George, V. L. Deringer, G. Hautier and R. Dronskowski, *J. Comput. Chem.*, 2020, **41**, 1931–1940.

(11) C. F. Bunge, J. A. Barrientos and A. V. Bunge, *At. Data Nucl. Data Tables*, 1993, **53**, 113–162.